Journal of Power Sources 182 (2008) 609–615

Contents lists available at ScienceDirect

Journal of Power Sources

journal homepage: www.elsevier.com/locate/jpowsour

Studies on a two-staged micro-combustor for a micro-reformer integrated with a micro-evaporator

K.B. Kim, O.C. Kwon*

School of Mechanical Engineering, Sungkyunkwan University, 300 Chunchun-dong, Jangan-gu, Suwon, Kyunggi-do 440-746, Republic of Korea

ARTICLE INFO

Article history:
Received 4 January 2008
Received in revised form 7 April 2008
Accepted 11 April 2008
Available online 30 April 2008

Keywords:
Micro-combustor
Micro-reformer
Micro-evaporator
Stability limits
Fuel cell

ABSTRACT

A new micro-combustor configuration for a micro fuel-cell reformer integrated with a micro-evaporator is studied experimentally and computationally. The micro-combustor as a heat source is designed for a 10–15 W micro-reformer using the steam reforming method. In order to satisfy the primary requirements for designing a micro-combustor integrated with a micro-evaporator, i.e., stable burning in a small confinement and maximum heat transfer through a wall, the present micro-combustor is a simply cylinder, which is easy to fabricate, but is two-staged (expanding downstream) to control ignition and stable burning. The aspect ratio and wall thickness of the micro-combustor substantially affect ignition and thermal characteristics. For optimized design conditions, a pre-mixed micro-flame is easily ignited in the expanded second-stage combustor, moves into the smaller first-stage combustor, and finally is stabilized therein. The measured and predicted temperature distributions across the micro-combustor walls indicate that heat generated in the micro-combustor is well transferred. Thus, the present micro-combustor configuration can be applied to practical micro-reformers integrated with a micro-evaporator for use with fuel cells.

1. Introduction

Direct methanol fuel cells (DMFCs) have been considered one of the most feasible portable power generation systems that may replace present lithium-ion batteries [1]. Recently, however, miniaturizing proton-exchange membrane fuel cells (PEMFCs) integrated with a liquid fuel and steam reforming system is found to have an advantage over micro DMFCs in terms of power density [2].

A micro-combustor as a heat source is required not only for the micro (or miniature) reformer since a catalytic processor of the reformer converts fed fuel and water steam into hydrogen (H_2) through an endothermic reaction but also for a micro-evaporator since liquid fuel and water should be vapourized. Due to the limited space in a micro system, the micro-combustor, the micro-reformer and the micro-evaporator should be compactly integrated with each other. Thus, guaranteeing stable burning in the micro-combustor, while effectively transferring heat into the reformer reactor and the evaporator, is one of the most important design aspects in developing a micro system for fuel reforming. Burning at the micrometer or millimeter scale imposes considerable technological challenges, particularly with respect to flame quenching.

Recently, there have been some fundamental studies on the design of micro-combustors [3–11]. Most studies have focused on catalyst-coated micro-combustors since they can easily sustain the burning with simple configurations [3–7]. When catalysts are used to assist combustion, however, their surface is easily poisoned; thus, it is expected that they face technological challenges, such as maintenance and durability, when they are applied in micro systems. In order to avoid flame quenching without catalysts in small confinements, heat-recirculating Swiss-roll combustors were introduced [8,9]. For minimizing heat losses to the surroundings, the heat-recirculation concept seems to be very effective. However, it is expected that the configurations of micro systems become complicated when the micro-combustors are integrated with other components such as evaporators and reformer reactors, to which heat should be effectively transferred. Another suggested approach to stabilizing flames without catalysts in small confinements is to use a vortex, particularly for non-premixed combustors for use in small-scale propulsion systems [10]. Prior to developing specific configurations of micro-combustors, however, experimental and computational investigations on the fundamental characteristics of combustion and heat transfer in a simplified configuration of confinement are needed for designing stably burning and heat transferring micro-combustors. Hua et al. [11] proposed a structure of pre-mixed hydrogen–air micro-flames in micro-scaled chambers, and focused on the effects of heat losses to the wall with micro-flames. The practical use of hydrogen for micro-combustors

* Corresponding author. Tel.: +82 31 290 7465; fax: +82 31 290 5889.
E-mail address: okwon@skku.edu (O.C. Kwon).

0378-7753/$ – see front matter © 2008 Elsevier B.V. All rights reserved.
doi:10.1016/j.jpowsour.2008.04.053

Nomenclature

d	inner diameter (mm)
l	micro-combustor length (mm)
$\dot{q}''$	heat flux ($W\,m^{-2}$)
r	radial coordinate
t	wall thickness (mm)
T	temperature (K)
V	micro-combustor inlet velocity ($m\,s^{-1}$)
x	axial coordinate
X_f	mole fraction of fuel
ϕ	fuel-equivalence ratio
γ	aspect ratio of each stage of micro-combustor

Subscripts

in	micro-combustor inlet
l	stability limits
w	wall of micro-combustor
1	the first stage of micro-combustor
2	the second stage of micro-combustor

however, is somewhat questionable due to the fuel storage problem, though hydrogen seems to have a less quenching feature compared with hydrocarbon fuels.

The detailed structure of micro-flames in a small confinement, including distributions of fuel and temperature, can enhance the understanding of the mechanism of micro-combustion. In order to accurately predict the micro-flame structure, two- or three-dimensional simulations are required, whereas most numerical studies for various basic combustion phenomena have been accomplished through one-dimensional simulations. This is because the simulations include a detailed or reduced reaction mechanism and because detailed reaction and transport modelling demands tremendous computation time [12]. In addition, given that it is technologically challenging to ignite gaseous reactants in a small confinement under cold conditions, a method to ignite easily the reactants and then to stabilize the burning should be considered.

In view of the above considerations, in the present investigation we aim to design a new micro-combustor configuration (as simple as possible) without catalysts for a micro fuel-cell reformer integrated with a micro-evaporator, with the following specific objectives. The first is to determine a basic configuration of the micro-combustor that can feasibly control ignition and stable burning for a 10–15 W micro-reformer using the steam reforming process. The second is to determine the stability limits of mass flow rates (or inlet velocities) and fuel concentration (or fuel-equivalence ratios) of supplied hydrocarbon–air pre-mixtures for stable burning and heat transfer. The third is to observe the effects of geometric variations such as aspect ratio and wall thickness of the micro-combustor on stability limits in the micro-combustor and heat transfer through the combustor walls. The fourth is to identify the optimized design conditions from the observations. We shall also examine the structure of the micro-flame in the small confinement, based on computational fluid dynamics (CFD) simulation with a simplified kinetic mechanism, in order to gain more understanding about some unique characteristics of micro-flames and heat transfer through the walls.

The basic configuration of the micro-combustor, the stability limits of mass flow rates and fuel concentration of supplied hydrocarbon–air pre-mixtures for stable burning, the effects of geometric variations on combustion and heat transfer characteristics, and the optimized design conditions will be subsequently presented, following the specification of the experimental and computational methods used during the present investigation.

2. Experimental and computational methods

A diagram of the present experimental apparatus is given in Fig. 1. The set-up consists of a test micro-combustor (stainless steel, SS304), a fuel–air mixture supply system, and thermocouples for measuring temperature distribution on the surface of the outer wall of the micro-combustor. Commercial mass flow controllers (Teledyne Hasting Instruments: 5, 10, 50 and 100 sccm) with an accuracy of ±0.75% of full-scale delivers the combustible mixture to the tube. The controllers are managed by a PC-based software (LabVIEW) that enables independent control of mixture composition (fuel-equivalence ratio ϕ) and micro-combustor inlet velocity V. The temperature distribution on the surface of the outer wall surface of the micro-combustor is measured using K-type thermocouples (a bead diameter of $250 \pm 20\,\mu m$) with an accuracy of ±0.05%. The test micro-combustors are two-staged; detailed configurations of the designed micro-combustors will be discussed later.

Flames in the micro-combustors were obtained by establishing a downward-injected, cold flow of reactive mixture that was then ignited in the second-stage micro-combustor with a spark. Once the mixture is ignited, flames moved backward and were stabilized in the first-stage micro-combustor having a smaller diameter than that of the second-stage micro-combustor. Experiments were carried out for propane (C_3H_8, purity > 99.9%)–air ($21\%O_2/79\%N_2$ in volume) mixtures of $\phi = 0.6$–1.5 and $V = 0.65$–$1.00\,m\,s^{-1}$ at a temperature $T = 298 \pm 3$ K and atmospheric pressure (normal temperature and pressure, NTP). Propane was chosen as fuel since it can be liquefied at relatively low pressures, be easily vapourized when mixed with air at NTP and be more readily ignited than natural gas. Thus, propane has a potential in practical use. Stability limits and temperature distribution on the outer wall surface of the micro-combustor were measured. All measurements were conducted for fixed inner diameters of the first and second-stage micro-combustors, namely, $d_1 = 2.5$ and $d_2 = 3.2$ mm, respectively. To evaluate the effects of the aspect ratio of each stage (γ_i, $i = 1$ and 2 for the first stage and the second stage, respectively) and the wall thickness (t_w) of the micro-combustors on the micro-combustor performance, the experiments were carried out for micro-combustors with $\gamma_1 = 2.0$–4.0, $\gamma_2 = 1.6$ and $t_w = 0.5$–1.5 mm.

The micro-combustion was simulated using a commercially available CFD code FLUENT 6.2 [13], the results from which were analyzed along with those of experimental tests for effectively designing micro-combustors. The time-dependent ordinary sets of the continuity equation, the cylindrical two-dimensional (cylindrical: r–x, where r and x are the radial and axial coordinates,

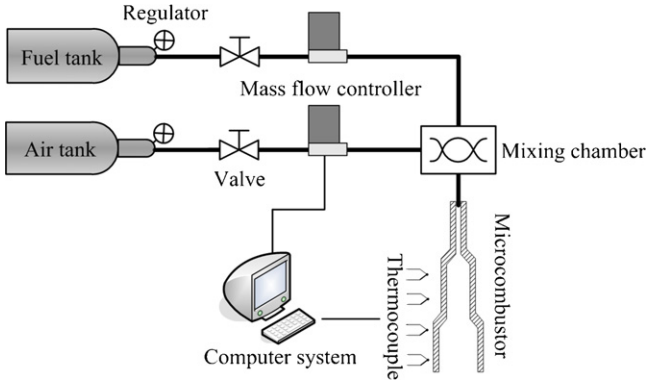

Fig. 1. Schematic of experimental apparatus.

respectively) Navier-Stokes equations, the energy conservation equation and the species conservation equations were solved via the finite volume method. The code allows for multi-component diffusion, thermal diffusion, variable thermochemical properties and variable transport properties. The CHEMKIN database was used to find the thermochemical properties [14]. Heat losses into the ambient air were considered but thermal radiation was negligible. Propane and air (21%O_2/79%N_2 in volume) mixtures were considered with a simplified 4-step reversible C_3H_8/O_2 reaction mechanism involving seven species due to Hautman et al. [15].

The governing equations adapting the above sub-models were discretized and simultaneously solved [13]. The entire region of calculations is $10d_1$ and $12d_1$ for the radial and axial directions, respectively (total number of 20,000 grid points). The parallel computation system consisted of 16 personal computers (CPU speed of 3.0 GHz each) allowed for the two-dimensional computations with the sub-models. Numerical simulations were conducted for the same conditions as those for the experiments.

3. Results and discussion

3.1. Micro-combustor configurations

In the present study a micro-combustor configuration for a 10–15 W micro-reformer using a steam reforming process is designed. Assuming that the conversion efficiencies of thermal and chemical to electric energies in a micro fuel-cell integrated with a micro-reformer and a micro-evaporator are much lower than those of a conventional macro-scale system, the size of the micro-combustor was determined.

In order to use a simple structured, but intensively heat-transferring, micro-combustor, a cylindrical configuration was chosen as the basic geometry of the micro-combustor. As the diameter of the micro-combustor decreases, the heat transfer into the reformer and the evaporator can be enhanced due to an increased surface-to-volume ratio. It will be more difficult, however to ignite the micro-combustor with the reduced size. Thus, a cylindrical, two-staged (expanding downstream) micro-combustor is suggested to control ignition and stable burning. Fig. 2 shows a basic micro-combustor configuration and major dimensions (d_1 = 2.5 mm, d_2 = 3.2 mm, γ_1 = 3.0, γ_2 = 1.6 and t_w = 0.5 mm) along with a conceptual design of a micro-reformer system integrated with the micro-combustor and a micro-evaporator. The coordinates used in the present investigation are also indicated. A pre-mixed micro-flame can be easily ignited in the expanded second-stage combustor since the diameter is larger than a typical quenching distance for hydrocarbon–air mixtures at NTP. Once the flame is generated in the second-stage micro-combustor, the first-stage micro-combustor is heated and then the flame is moved into the smaller first-stage combustor, finally stabilized therein, without any catalysts and preheating from an additional energy source. The present design concerns only the micro-combustor configuration (not the whole micro fuel-cell reformer system), thus experiments and computations were carried out for the micro-combustor surrounded by an atmosphere at NTP.

The virtual micro-reformer system in Fig. 2 shows the micro-reformer reactor and the micro-evaporator integrated annularly with the micro-combustor. For practical applications, however, various arrangements are possible, e.g., a micro-combustor surrounded with multiple tubes of micro-reformers and the micro-evaporators. The wall surface temperature distribution of the second-stage micro-combustor in the present micro-reformer system should be as uniform as possible since it is surrounded by the reformer reactor that requires a small temperature gradient

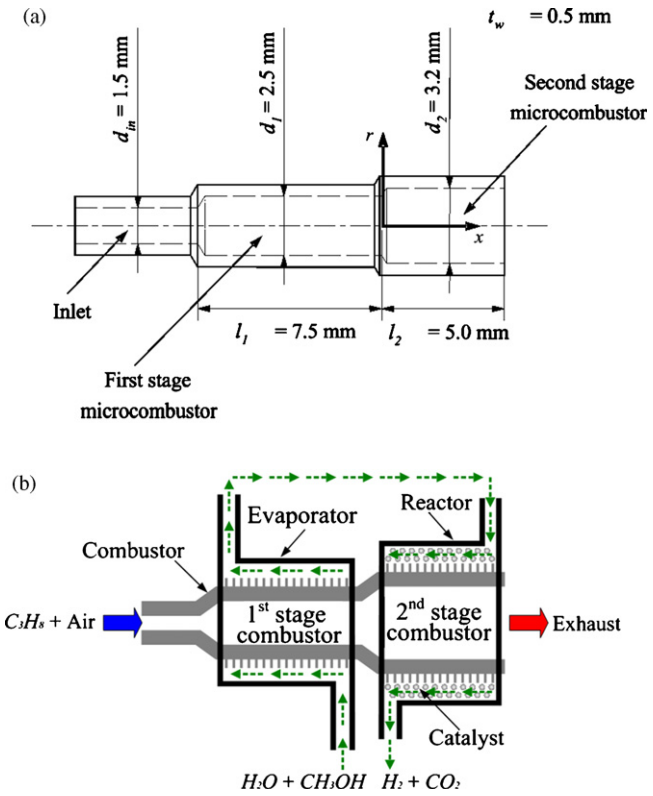

Fig. 2. Configuration of (a) two-staged micro-combustor and (b) conceptual design of micro-combustor integrated with micro-reformer and micro-evaporator.

along the wall for better performance. This requirement can be satisfied with the present micro-combustor configuration, as shown in Fig. 3 that gives the temperature distribution along the outer wall surface of the two-staged micro-combustor shown in Fig. 2 for a propane–air mixture of ϕ = 0.9 and V = 0.79 m s^{-1} at NTP. The mixture composition and inlet velocity are determined for stable burning conditions. Predicted distributions of the temperature and the mole fraction of fuel (X_f) in the micro-combustor are presented in Fig. 4. The location of the peak temperature is not accurately predicted and the temperature is somewhat

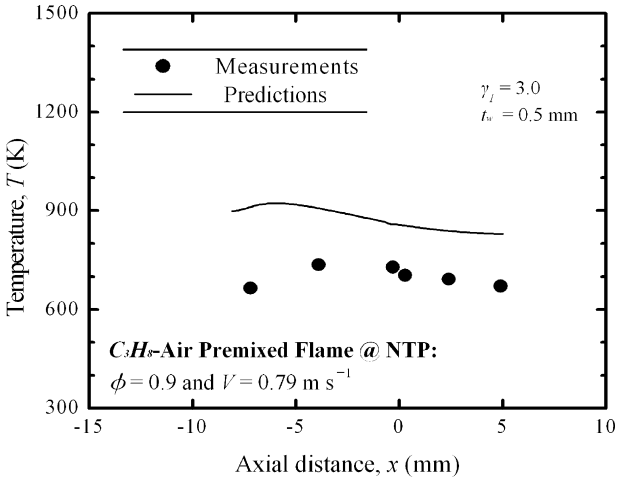

Fig. 3. Measured and predicted temperature distribution along outer wall surface of micro-combustor (d_1 = 2.5 mm, d_2 = 3.2 mm, γ_1 = 3.0, γ_2 = 1.6 and t_w = 0.5 mm) for propane–air mixture of ϕ = 0.9 and V = 0.79 m s^{-1} at NTP. Predictions based on reaction mechanism due to Hautman et al. [15].

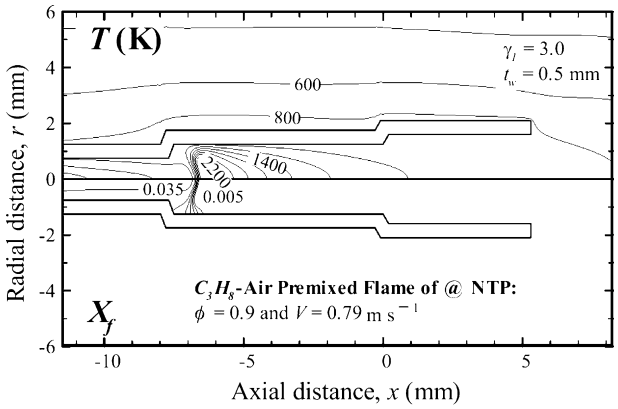

Fig. 4. Predicted distributions of temperature and mole fraction of fuel in micro-combustor (d_1 = 2.5 mm, d_2 = 3.2 mm, γ_1 = 3.0, γ_2 = 1.6 and t_w = 0.5 mm) for propane–air mixture of ϕ = 0.9 and V = 0.79 m s^{-1} at NTP. Based on reaction mechanism due to Hautman et al. [15].

overestimated in the whole micro-combustor; but, the measured tendency and temperature drop along the micro-combustor are well predicted computationally, which justifies the present micro-combustor design combining measurements with computations. The predicted distribution of fuel concentration shows that fuel starts to be consumed upstream of the first-stage micro-combustor and immediately disappears, implying that the residence time of the supplied mixture in the first-stage micro-combustor is long enough for localized burning. Finally, Fig. 5 shows the predicted radial heat fluxes through the wall for the baseline condition of Figs. 3 and 4. The amount of heat flux along with temperature in Fig. 3 seems to be reasonable for evaporating liquid fuel (e.g., methanol) and water and for reforming the vapourized mixture in the reformer reactor [16].

3.2. Stability limits of fuel–air pre-mixtures for stable burning

The stability limits of inlet velocities and fuel-equivalence ratios (V–ϕ) of supplied propane–air pre-mixtures for stable burning were determined by spark-igniting a cold mixture in the second-stage micro-combustor, observing steady-state burning in the first-stage micro-combustor, and then decreasing or increasing the

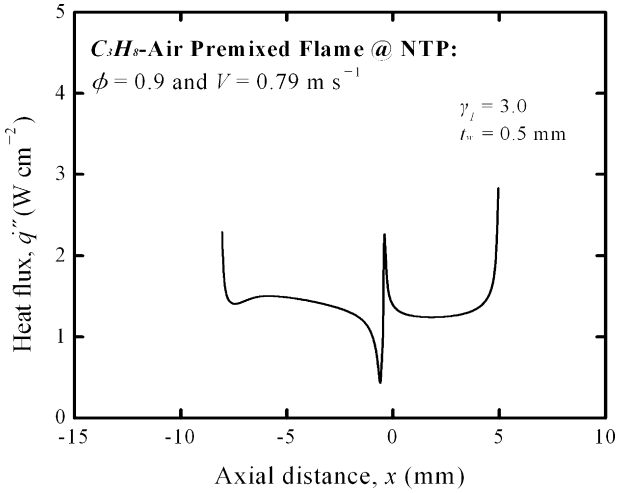

Fig. 5. Predicted radial heat fluxes through wall of micro-combustor (d_1 = 2.5 mm, d_2 = 3.2 mm, γ_1 = 3.0, γ_2 = 1.6 and t_w = 0.5 mm) for propane–air mixture of ϕ = 0.9 and V = 0.79 m s^{-1} at NTP. Predictions based on reaction mechanism due to Hautman et al. [15].

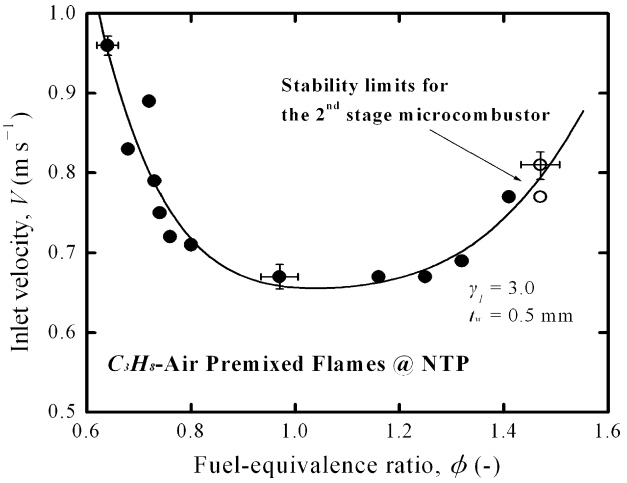

Fig. 6. Stability limits of pre-mixed propane–air flames in V–ϕ space for micro-combustor of d_1 = 2.5 mm, d_2 = 3.2 mm, γ_1 = 3.0, γ_2 = 1.6 and t_w = 0.5 mm.

fuel concentration until the steady-state operation ceased. Also, measurements of the stability limits at high Vs were stopped once flames were established outside the micro-combustor. These limits were independent of the path in the V–ϕ space used to reach the limit. The Vs are area-averaged on the inlet of the micro-combustor.

The stability limits for the baseline configuration of the micro-combustor in Fig. 2 (d_1 = 2.5, d_2 = 3.2 mm and t_w = 0.5 mm) are given in Fig. 6. It should be noted that there are two stability limits: one for the first-stage micro-combustor and the other for the second-stage micro-combustor. For the conceptual arrangement of a micro-combustor integrated with a micro-reformer and a micro-evaporator in Fig. 2, only the limit for the first-stage micro-combustor is meaningful in practice. Thus, the stability limits only for the first-stage micro-combustor will be displayed hereafter. Error bars for some data points indicate typical variations for the present measurements of the stability limits. Similar to stability limits for meso (or macro) scale combustors [8], fuel-lean and fuel-rich stability limits are observed. At relatively high Vs, the stability limit fuel-equivalence ratio ϕ_l changes slightly as V increases, while at low Vs, ϕ_l changes considerably as V decreases. These limits correspond to insufficient residence time limits and heat loss limits, respectively [8]. This tendency is observed since heat loss rates are almost independent of the Vs, but heat release rates are proportional to mass flow rates (thus Vs). It is observed that the stability limits change more rapidly for the fuel-lean region than for the fuel-rich region, though the minimum stability V is found near the stoichiometric condition (ϕ = 1). This is observed due to the definition of ϕ, unsymmetrically scaling the fuel-to-oxygen ratio for fuel-lean (0–1) and fuel-rich (1–∞) conditions.

3.3. Effects of geometric variations

Experiments were systematically conducted to investigate the effect of the aspect ratios of the first-stage micro-combustor and the micro-combustor wall thickness on (i) the stability limits for stable burning and (ii) the temperature distribution along the micro-combustor wall for effective heat transfer.

The effect of the aspect ratio of the first-stage micro-combustor on the stability limits for stable burning are shown in Fig. 7. The experiments were conducted for micro-combustors of γ_1 = 2.0, 3.0 (the baseline configuration shown in Fig. 2) and 4.0 and γ_2 = 1.6 (d_1 = 2.5, d_2 = 3.2 mm and t_w = 0.5 mm). An optimized value of γ_2 was determined through repeated ignition experiments for various test conditions; thus, the value of γ_2 is fixed in the present

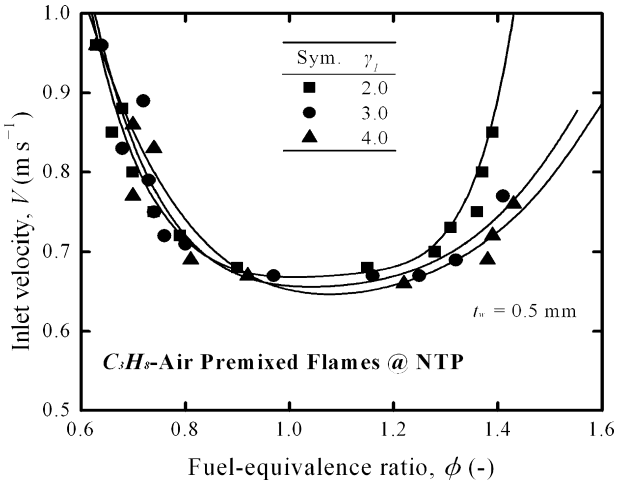

Fig. 7. Effects of γ_1 on stability limits of pre-mixed propane–air flames in V–ϕ space for micro-combustors of d_1 = 2.5 mm, d_2 = 3.2 mm, γ_2 = 1.6 and t_w = 0.5 mm: γ_1 = 2.0, 3.0 and 4.0.

investigation. The stability limits are extended with increasing γ_1: similar for fuel-lean limits but substantially extended for fuel-rich limits. This tendency is observed since the residence time of a supplied mixture increases with increasing γ_1, because the fuel is more completely consumed in the first-stage micro-combustor. This observation also explains why the stability limits are not sensitive to γ_1 for fuel-lean conditions. Thus, stable combustion in the micro-combustor is most favourable at enhanced aspect ratios of the first-stage micro-combustor within the length allowed for space and integration with the micro-reformer reactor and the micro-evaporator.

The effects of the aspect ratios of the first-stage micro-combustors on the temperature distribution along the micro-combustor wall are shown in Fig. 8. The experiments were conducted for a propane–air mixture of ϕ = 0.9 and V = 0.79 m s^{-1} at NTP (the baseline condition of Fig. 3) in micro-combustor of γ_1 = 2.0, 3.0 (the baseline configuration shown in Fig. 2) and 4.0. Predicted distributions of temperature and mole fraction of fuel in the micro-combustors for γ_1 = 2.0 and 4.0 are shown in Fig. 9. The temperature in the second-stage micro-combustor decreases with increasing γ_1, due to the enhanced total amount of heat transfer

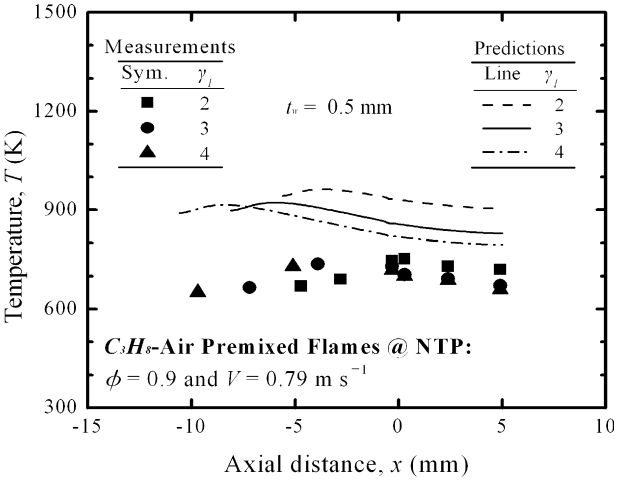

Fig. 8. Effects of γ_1 on temperature distribution along outer wall surface of micro-combustors (d_1 = 2.5 mm, d_2 = 3.2 mm, γ_2 = 1.6 and t_w = 0.5 mm) for propane–air mixture of ϕ = 0.9 and V = 0.79 m s^{-1} at NTP: γ_1 = 2.0, 3.0 and 4.0. Predictions based on reaction mechanism due to Hautman et al. [15].

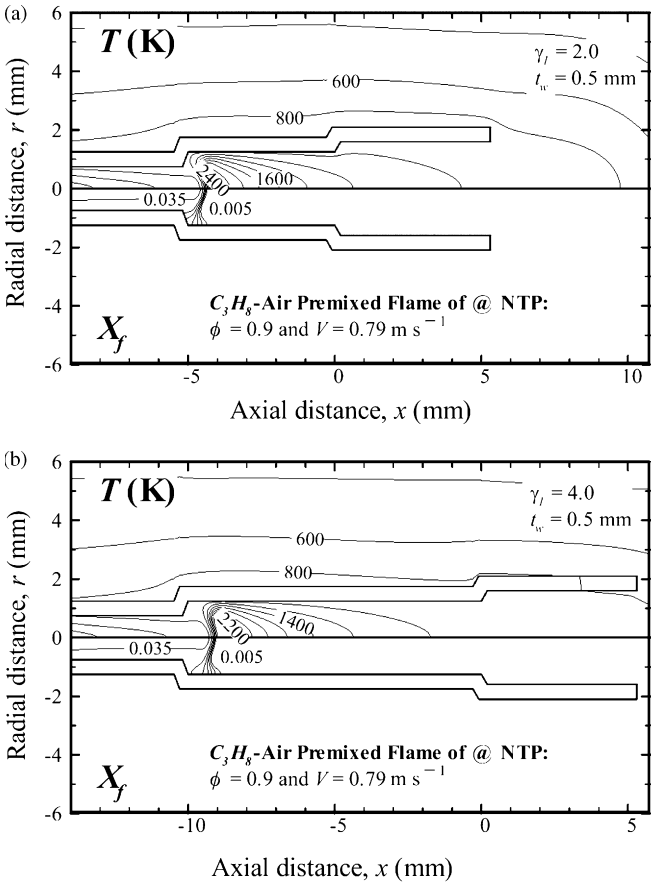

Fig. 9. Effects of γ_1 on distributions of temperature and mole fraction of fuel in micro-combustors (d_1 = 2.5 mm, d_2 = 3.2 mm, γ_2 = 1.6 and t_w = 0.5 mm) for propane–air mixture of ϕ = 0.9 and V = 0.79 m s^{-1} at NTP: (a) γ_1 = 2.0 and (b) 4.0. Predictions based on reaction mechanism due to Hautman et al. [15].

through the wall in the first-stage micro-combustor. The temperature uniformity in the second-stage micro-combustor is similar for various γ_1s. In the first-stage micro-combustor, the peak temperature decreases again due to the enhanced total amount of heat transfer through the micro-combustor wall and the location of the peak temperature shifts relatively upstream due to the enhanced residence time of the supplied mixture in the first-stage micro-combustor with increasing γ_1. All these measured tendencies are well predicted computationally. On the other hand, the location of the peak temperature is not accurately predicted and results in an overestimate of temperature in the whole micro-combustor. Fig. 10 shows that radial heat fluxes through the micro-combustor wall are reduced with increasing γ_1 and that they can be controlled over a wide range, with just a relatively small variation of γ_1. It should be noted, however, that the effects of γ_2 variation on the radial heat fluxes are less significant (not shown here), though the tendency is similar to that of γ_1. Thus, in the present study, γ_2 was fixed at the optimized value determined through repeated ignition experiments for various test conditions, as described earlier.

The effects of micro-combustor wall thickness on the stability limits for stable burning are shown in Fig. 11. The experiments were conducted for micro-combustors of t_w = 0.5 (the baseline configuration shown in Fig. 2) and 1.5 mm (d_1 = 2.5, d_2 = 3.2 mm, γ_1 = 3.0 and γ_2 = 1.6). The stability limits are extended with decreasing t_w, though the effects on the stability limits are less significant compared with those of γ_1 (shown in Fig. 7). This tendency implies that heat conduction in the axial direction plays an important role in the micro-combustor. Since the axial heat losses compared with the

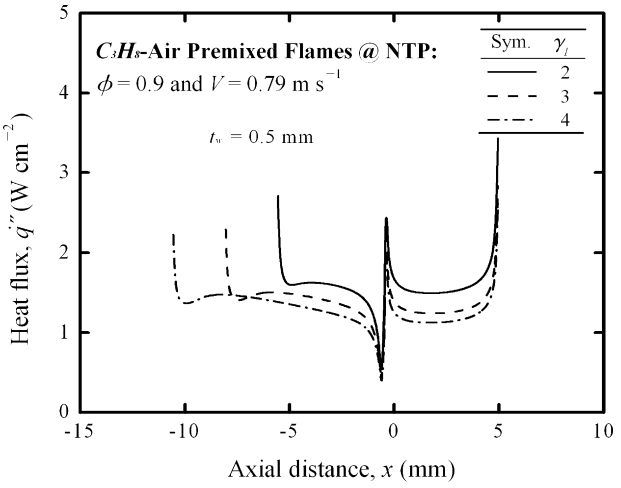

Fig. 10. Effects of γ_1 on radial heat fluxes through wall of micro-combustors (d_1 = 2.5 mm, d_2 = 3.2 mm, γ_2 = 1.6 and t_w = 0.5 mm) for propane–air mixture of ϕ = 0.9 and V = 0.79 m s^{-1} at NTP: γ_1 = 2.0, 3.0 and 4.0. Predictions based on reaction mechanism due to Hautman et al. [15].

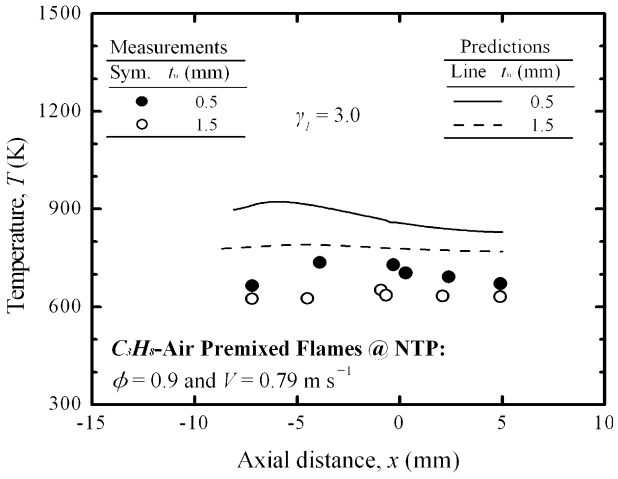

Fig. 12. Effects of t_w on temperature distribution along outer wall surface of micro-combustors (d_1 = 2.5 mm, d_2 = 3.2 mm, γ_1 = 3.0 and γ_2 = 1.6) for propane–air mixture of ϕ = 0.9 and V = 0.79 m s^{-1} at NTP: t_w = 0.5 and 1.5 mm. Predictions based on reaction mechanism due to Hautman et al. [15].

radial heat transfer across the wall increase with increasing t_w, the stability limits are reduced. This suggests that stable combustion in the micro-combustor is most favourable at thinner walls within the thickness allowed for fabrication and structural strength. Estimates of the axial heat losses will be discussed later.

The effects of micro-combustor wall thickness on the temperature distribution along the wall are shown in Fig. 12. The experiments were conducted for a propane–air mixture of ϕ = 0.9 and V = 0.79 m s^{-1} at NTP (the baseline condition of Fig. 3) in micro-combustors of γ_1 = 3.0 and t_w = 0.5 (the baseline configuration shown in Fig. 2) and 1.5 mm. Predicted distributions of temperature and the mole fraction of fuel in the micro-combustor for t_w = 1.5 mm are presented in Fig. 13. Temperature in the whole micro-combustor decreases but the temperature uniformity in the second-stage micro-combustor is substantially enhanced with increasing t_w. This tendency again implies that heat conduction in the axial direction plays an important role in the micro-combustor. Since the enhanced axial heat conduction compared with the radial heat transfer across the wall with increasing t_w redistributes heat along the wall, the temperature uniformity is enhanced, and thereby reduces the peak temperature. This measured tendency is well predicted computationally; however, temperature in the whole micro-combustor is overestimated. Finally, Fig. 14 confirms that radial heat fluxes through the micro-combustor wall are reduced with increasing t_w, due to increasing axial heat losses at the outlet edge of the second-stage micro-combustor, as well as to increasing area of the outer wall surface.

The axial heat conduction losses along the micro-combustor wall can be estimated from the predicted temperature distribution, as shown in Figs. 4, 9 and 13. Under the present test conditions, the axial heat losses compared with the radial heat transfer across the wall vary from 2.7 to 6.4%, increasing with increasing t_w. This tendency is expected since a simple analysis of heat conduction in the micro-combustor wall using the energy conservation equation can show that the relative losses are proportional to $(t_w/d)^2$. Greater heat losses with increasing t_w are also confirmed from the measured gas temperature at the exit of the second-stage micro-combustor, i.e., 668 and 655 K for micro-combustors with t_w = 0.5 and 1.5 mm, respectively.

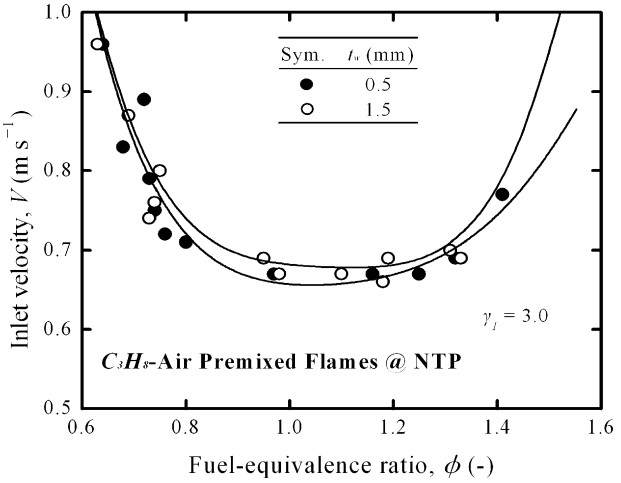

Fig. 11. Effects of t_w on stability limits of pre-mixed propane–air flames in V–ϕ space for micro-combustors of d_1 = 2.5 mm, d_2 = 3.2 mm, γ_1 = 3.0 and γ_2 = 1.6: t_w = 0.5 and 1.5 mm.

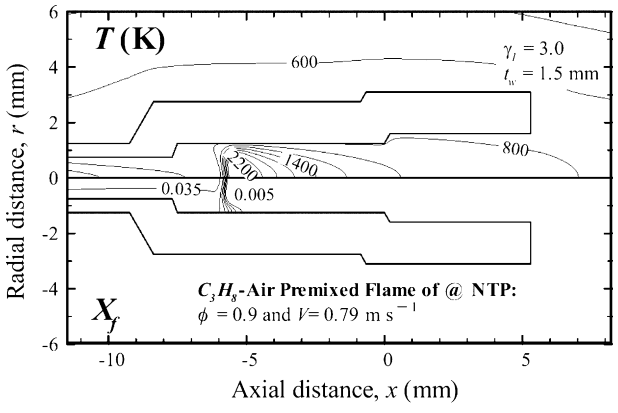

Fig. 13. Effects of t_w on distributions of temperature and mole fraction of fuel in micro-combustors (d_1 = 2.5 mm, d_2 = 3.2 mm, γ_1 = 3.0 and γ_2 = 1.6) for propane–air mixture of ϕ = 0.9 and V = 0.79 m s^{-1} at NTP: t_w = 1.5 mm. Predictions based on reaction mechanism due to Hautman et al. [15].

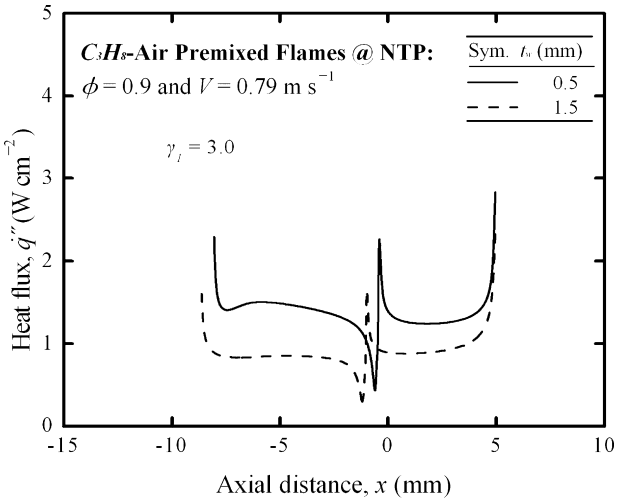

Fig. 14. Effects of t_w on radial heat fluxes through wall of micro-combustors (d_1 = 2.5 mm, d_2 = 3.2 mm, γ_1 = 3.0 and γ_2 = 1.6) for propane–air mixture of ϕ = 0.9 and V = 0.79 m s^{-1} at NTP: t_w = 0.5 and 1.5 mm. Predictions based on reaction mechanism due to Hautman et al. [15].

3.4. Optimized design conditions

So far we have investigated the effects of geometric variations on the performance of a two-staged micro-combustor. For a given fuel-equivalence ratio and inlet velocity of a supplied mixture, it is considered that stable burning in the first-stage micro-combustor is most favourable at (i) enhanced aspect ratios of the first-stage micro-combustor within a proper range of radial heat flux and temperature on the outer wall surface that allows fuel and water evaporation and fuel reforming processes, and (ii) thinner walls within the allowable thickness for fabrication and structural strength. For uniform temperature distribution on the outer wall surface of the second-stage micro-combustor, however, thicker walls are preferred within the range of radial heat flux and temperature on the outer wall surface that is required for fuel and water vapourizing and fuel reforming processes. Thus, depending on the priority of the major performance parameters of the micro-combustor, the wall thickness should be precisely designed. For example, if the temperature uniformity is more emphasized assuming that all the present test conditions and configurations of micro-combustors are allowed for operating the virtual micro fuel reforming system shown in Fig. 2, the optimized design condition is to burn a propane–air mixture of ϕ = 0.9 and V = 0.79 m s^{-1} at NTP in micro-combustors of γ_1 = 3.0 and t_w = 1.5 mm.

Finally, it should be noted that further considerations are needed to obtain a fully optimized design condition, e.g., materials of the micro-combustor.

4. Concluding remarks

A new micro-combustor configuration for a micro fuel-cell reformer integrated with a micro-evaporator has been studied experimentally and computationally. The micro-combustor as a heat source is designed for a 10–15 W micro-reformer using a steam reforming process. The major conclusions of the study are as follows.

1. In order to satisfy the primary requirements for designing a micro-combustor integrated with a micro-evaporator, i.e., stable burning in a small confinement and maximum heat transfer through a wall, the present micro-combustor is cylindrical and therefore easy to fabricate, but is two-staged (expanding downstream) to control ignition and stable burning.
2. For the optimized design conditions, a pre-mixed micro-flame is easily ignited in the expanded second-stage combustor, moved into the smaller first-stage combustor, and finally stabilized therein.
3. The measured and predicted temperature distributions across the micro-combustor walls indicate that heat generated in the micro-combustor is well transferred. Thus, the present micro-combustor configuration can be applied to practical micro-reformers integrated with a micro-evaporator for use with fuel cells.
4. The limits for stable burning in the micro-combustor are substantially extended with increasing aspect ratios of the first-stage micro-combustor.
5. The stability limits are extended, but the temperature uniformity along the micro-combustor wall is somewhat degraded, with decreasing wall thickness of the micro-combustor. Thus, an optimized condition should be determined depending on the priority among major performance parameters for a given micro fuel processing system.

Acknowledgement

This work was supported by the Korea Energy Management Corporation, Korea under Grant No. 2004-03-0012-0-000.

References

[1] G.Q. Lu, C.Y. Wang, J. Power Sources 144 (2005) 141–145.
[2] M. Shioya, 2nd Int. Hydrogen & Fuel Cell Expo, 2006, pp. 69–85.
[3] J.D. Holladay, E.O. Jones, R.A. Dagle, G.G. Xia, C. Cao, Y. Wang, J. Power Sources 131 (2004) 69–72.
[4] S.-K. Ryi, J.-S. Park, S.-H. Choi, S.-H. Cho, S.-H. Kim, Chem. Eng. J. 113 (2005) 47–53.
[5] T. Okamasa, G.-G. Lee, Y. Suzuki, N. Kasagi, S. Matsuda, J. Micromech. Microeng. 16 (2006) S198–S205.
[6] K. Yoshida, S. Tanaka, H. Hiraki, M. Esashi, J. Micromech. Microeng. 16 (2006) S191–S197.
[7] D.-E. Park, T. Kim, S. Kwon, C.-K. Kim, E. Yoon, Sens. Actuators A 135 (2007) 58–66.
[8] J. Ahn, C. Eastwood, L. Sitzki, P.D. Ronney, Proc. Combust. Inst. 30 (2005) 2463–2472.
[9] N.I. Kim, S. Aizumi, T. Yokomori, S. Kato, T. Fujimori, K. Maruta, Proc. Combust. Inst. 31 (2007) 3243–3250.
[10] M.-H. Wu, Y. Wang, V. Yang, R.A. Yetter, Proc. Combust. Inst. 31 (2007) 3235–3242.
[11] J. Hua, M. Wu, K. Kumar, Chem. Eng. Sci. 60 (2005) 3497–3506.
[12] O.C. Kwon, KSME Int. J. 18 (2004) 325–334.
[13] Fluent Inc., Fluent 6.2 User's Guide, Fluent Inc., Lebanon, 2001.
[14] R.J. Kee, F.M. Rupley, J.A. Miller, The CHEMKIN Thermodynamic Data Base, Albuquerque, NM, USA, Sandia National Laboratories Report SAND87-8215B, 1992.
[15] D.J. Hautman, F.L. Dryer, K.P. Schug, I. Glassman, Combust. Sci. Tech. 25 (1981) 219–235.
[16] J. Piña, V. Bucalá, D.O. Borio, Int. J. Chem. Reactor Eng. 1 (2003) A25.